

Short Communication

Pack Boronizing of P110 Oil Casing Tube Steel to Combat Wear and Corrosion

Naiming Lin^{1,*}, Peng Zhou¹, Hongwei Zhou², Junwen Guo¹, Hongyan Zhang¹, Jiaojuan Zou¹, Yong Ma¹, Pengju Han³, Bin Tang¹

¹ Research Institute of Surface Engineering, Taiyuan University of Technology, Taiyuan, 030024, P. R. China

² No. 52 Institute of China Ordnance Industries Group, Baotou 014034, P. R. China

³ Department of Civil Engineering, Taiyuan University of Technology, Taiyuan, 030024, P. R. China

*E-mail: lnmlz33@126.com

Received: 6 December 2014 / Accepted: 11 January 2015 / Published: 19 January 2015

In the present work, boronizing coating was produced by pack cementation to improve the surface performance and increase the usage lifetime of P110 oil casing tube steel during operation. Scanning electron microscope (SEM), X-ray diffraction (XRD) and glow discharge optical emission spectroscopy (GDOES) were used to investigate the surface morphology, cross-sectional microstructure, phase constitutions and element distribution of the boronizing coating. The wear and corrosion resistance of boronizing coating and P110 steel were evaluated on high speed reciprocating friction tester and electrochemical workstation, respectively. The results showed that the obtained coating was uniform and continuous, mainly consisted of Fe₂B and reached a thickness of 20 μm. The the wear and corrosion resistance of the P110 steel can be improved by boronizing coating. In conclusion, the formed coating has significantly improved the surface performance of P110 steel.

Keywords: Pack; boronizing; P110 steel; wear; mass loss; corrosion; potentiodynamic polarization; electrochemical impedance spectroscopy

1. INTRODUCTION

The economic growth around the world over the recent decades has resulted in a heavy increase in the consumption of oil/gas and other resources, causing the urgent need for many additional wells to exploit oil/gas resources [1, 2]. The oil casing tube is an important structural unit of the oil/gas well, considerable economic loss occurs because of corrosion and wear under complex and adverse operating conditions [3]. Carbon dioxide (CO₂) corrosion which is also referred to as “sweet corrosion” is a serious concern in the oil/gas production and transportation systems [3]. The CO₂

corrosion is a significant contributing factor that causes the degradation of casing tube. Besides, casing tubes also experience severe wear in the course of drilling. Besides the common wear damages which originate from the friction between the casing tube and the sucker rod (see Figure 1) [4]; wear damages also occur in the drilling of extended-reach wells, long horizontal traverse wells, horizontal wells and deep wells or in the intervals with great dogleg severity, as well as drilling the long open hole whose intermediate casings have been tripped in [5]. The wearing of casing tube can lead to the reduction of collapsing strength and internal pressure strength, and this can result in shortening the service lifetime of oil/gas wells, even the abandonment of a certain interval or the whole oil well [6]. The recent understanding of the degradation of oil casing tubes has led to the finding that the use of corrosion-resistant alloy tubes with high strength is an effective solution for increasing the life of the tubes [2]. However, most of the corrosion-resistant alloy tubes contain noble alloy elements, such as Ni, Cr, and Mo, which contribute significantly to an increase in cost.

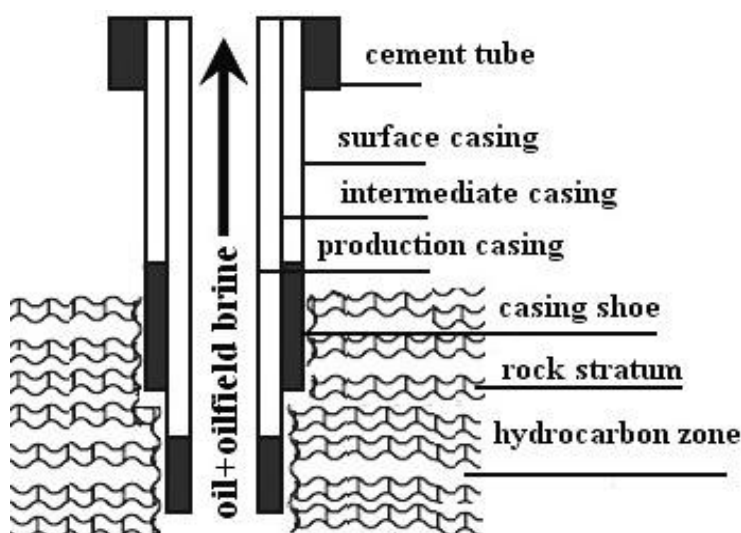


Figure 1. Open hole completion and well bore structure

For a compromise between cost and performance, surface engineering techniques have been applied to overcome the problems of corrosion, wear, and high temperature oxidation of materials. From a short-term benefit-cost view, using oil casing tube made of plain carbon steel is a cost-saving option [2]. Therefore, surface treatment is a convenient and effective method to improve the surface properties of plain carbon steel oil casing tube [7]. Boronizing is an in-situ thermo-chemical surface treatment process that involves diffusion of boron atoms into the surface of metal/alloy to produce a layer of borides of the corresponding metal/alloying elements [8]. Boronizing is able to simultaneously impart ferrous, non-ferrous and even some super alloys with high hardness, promising wear/corrosion resistance and ideal oxidation resistance [9]. Depending on the physical state of boronizing media, various boronizing methods have been developed: gas boronizing and liquid boronizing [10]. Because of its simpleness, practicality and low cost, powder pack cementation is the most commonly used [10]. However, little information exists in the literature on the application of boronizing on P110 steel.

In this work, in order to improve the surface corrosion and wear resistance of P110 steel, boronizing was conducted by powder pack cementation. The microstructure, chemical and phase compositions, and wear and corrosion resistance of the boronizing coatings and the substrate were investigated.

2. EXPERIMENTAL PROCEDURES

2.1. Material and boronizing process

The substrate material was cut into 20 mm × 20 mm × 3 mm plates from a P110 steel oil casing tube by a spark-erosion wire cutting machine. All the specimens were manually ground using 1000 grit SiC abrasive paper to get the final surface finish and then ultrasonically cleaned in acetone bath before boronizing treatment. The chemical compositions of the materials used in the experiments are given in Table 1. Pack boronizing process which is basically an in-situ, self generated chemical vapor deposition (CVD) process was preferred because of its ease of treatment, availability of a smooth surface, and simplicity of the required apparatus and equipment (see Figure 2) [8, 11]. An electric tube furnace was employed in the pack cementation process: (1) All the specimens were placed into the aluminide crucibles filled with LSB-IA; (2) the sealed crucibles were put into the furnace, which was heated to 150 °C and held at this temperature for 3 h to remove the moisture from the pack; (3) the furnace was raised up to and kept at the desired temperature of 950 °C for 5 h; and (4) the crucibles were taken out and cooled down to room temperature in air.

Table 1. Chemical composition of P110 steel (wt. %)

Element	C	Si	Mn	P	S	Cr	Ni	Mo	Cu	Nb	V	Ti	Fe
P110	0.26	0.19	1.37	0.009	0.004	0.148	0.028	0.013	0.019	0.06	0.006	0.011	Bal

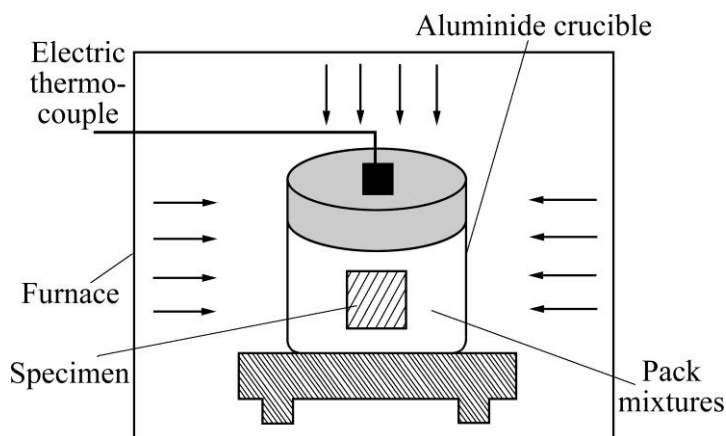


Figure 2. Schematic diagram of pack cementation device

2.2. Characterizations and testings

The surface morphology/cross-sectional microstructure of the boronizing coating and the topographical features of the worn surfaces belonging to the samples were examined using a scanning electron microscope (SEM). The concentration profile of the elements over the thickness of the boronizing coating was analyzed by glow discharge optical emission spectroscopy (GDOES). The phase constitution of the coating was identified by X-ray diffraction (XRD).

The wear resistance of the coating was evaluated on the high speed reciprocating friction tester, two counterparts (GCr15 and Si₃N₄ balls, 5 mm in diameter) were pressed under a load of 20 N against the surface of a boronized specimen for reciprocating motion. The travel distance was 5 mm, the reciprocating frequency was 2 Hz, and the wear test lasted for 30 min. An analytical balance with an accuracy of 0.01 mg was employed to weigh the original and worn samples.

Open circuit potential (OCP), potentiodynamic polarization and electrochemical impedance spectroscopy (EIS) were conducted to examine the corrosion resistance of the boronizing coating. CO₂-saturated simulated oilfield stratum water was selected as corrosion medium. The chemical composition of the corrosion medium is shown in Table 2 [12]. The experiments were performed with the electrochemical measurement system. The corrosion cell was combined with a conventional three-electrode configuration. A saturated calomel electrode (SCE, 0.242 V vs. SHE) was used as reference electrode and the counter electrode was a platinum auxiliary electrode. All the tests were conducted inside a thermostat at 303 K [12]. The polarization tests of the samples were performed after they had been soaked in the solution for 3600 s. Electrochemical impedance spectroscopy (EIS) was obtained at open circuit potential (E_{ocp}) in the frequency ranging from 100 kHz to 0.01 Hz, and the ac perturbation amplitude was 10 mV. All the electrochemical curves were plotted by using origin 8.0 program.

Table 2. Concentration of electrolyte in simulated oilfield stratum water

Content	Cl ⁻	SO ₄ ²⁻	HCO ₃ ⁻	CO ₃ ²⁻	Na ⁺	Mg ²⁺	Ca ²⁺
mg/L	19	1.14	0.6	0.12	11.99	1.05	0.39

3. RESULTS AND DISCUSSION

3.1. Microstructural characterizations

Figure 3a and Figure 3b have showed the cross-sectional and surface morphology of the formed coating on P110 steel. It is found that the boronizing coating is continuous and compact. The coating reaches a total thickness of about 20 μm according to the measuring scale. The XRD pattern of the boronizing coating has been illustrated in Figure 3c. It is demonstrated that the boronizing coating is mainly composed of Fe₂B. GDOES compositional depth profile is given in Figure 3d, it is displayed that B, C and Fe are the major elements of the boronizing coating. It presents that the concentration of B and C gradually decreases, while the concentration of Fe tends to increase from the surface to the

interior. The maximum content of B is nearly 10 %, according to the GDOES result. The thickness of the boronizing coating was approximately 20 μm , as derived from GDOES analysis of the cross-section. And this is in good agreement with the SEM observation in Figure 3a.

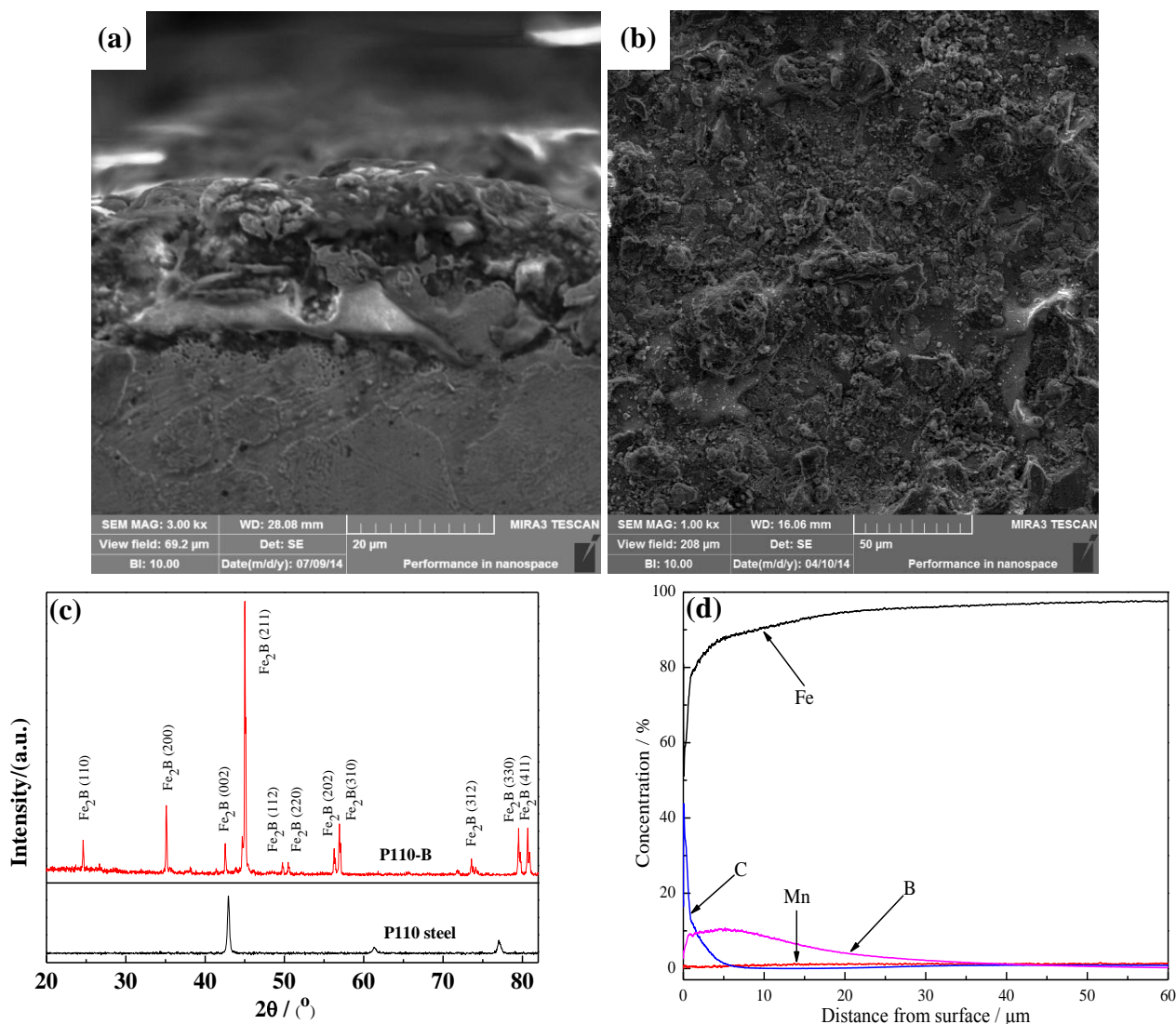


Figure 3. Microstructural characterizations of boronizing coating: (a) cross-sectional micrograph; (b) surface morphology; (c) X-ray diffraction pattern; (d) composition distribution

3.2. Wear resistance of boronizing coating

The wear scars of the coating and P110 steel substrate against GCr15 are shown in Figure 4. As presented in Figure 4a, the wear scar is continuous and complete, plastic deformation is evident on the worn surface of P110 steel. While the plastic deformation makes the adhesive wear increase [11, 13]. The higher magnified image in Figure 4b highlights the significant wear occurred during sliding. Worn surface of P110 steel is very rough, surface damages, such as adhesive craters and abrasive scoring marks were clearly observable. Thereby, the dominating wear mechanism of P110 steel is abrasive

wear combined with adhesive wear. Seen from Figure 4c and Figure 4d, the wear trace of the boronizing coating is incomplete and discontinuous. The wear mode of boronizing coating is mainly the adhesive transfer of GCr15 ball, which might be attributed the lower hardness of GCr15 in comparison with the coating.

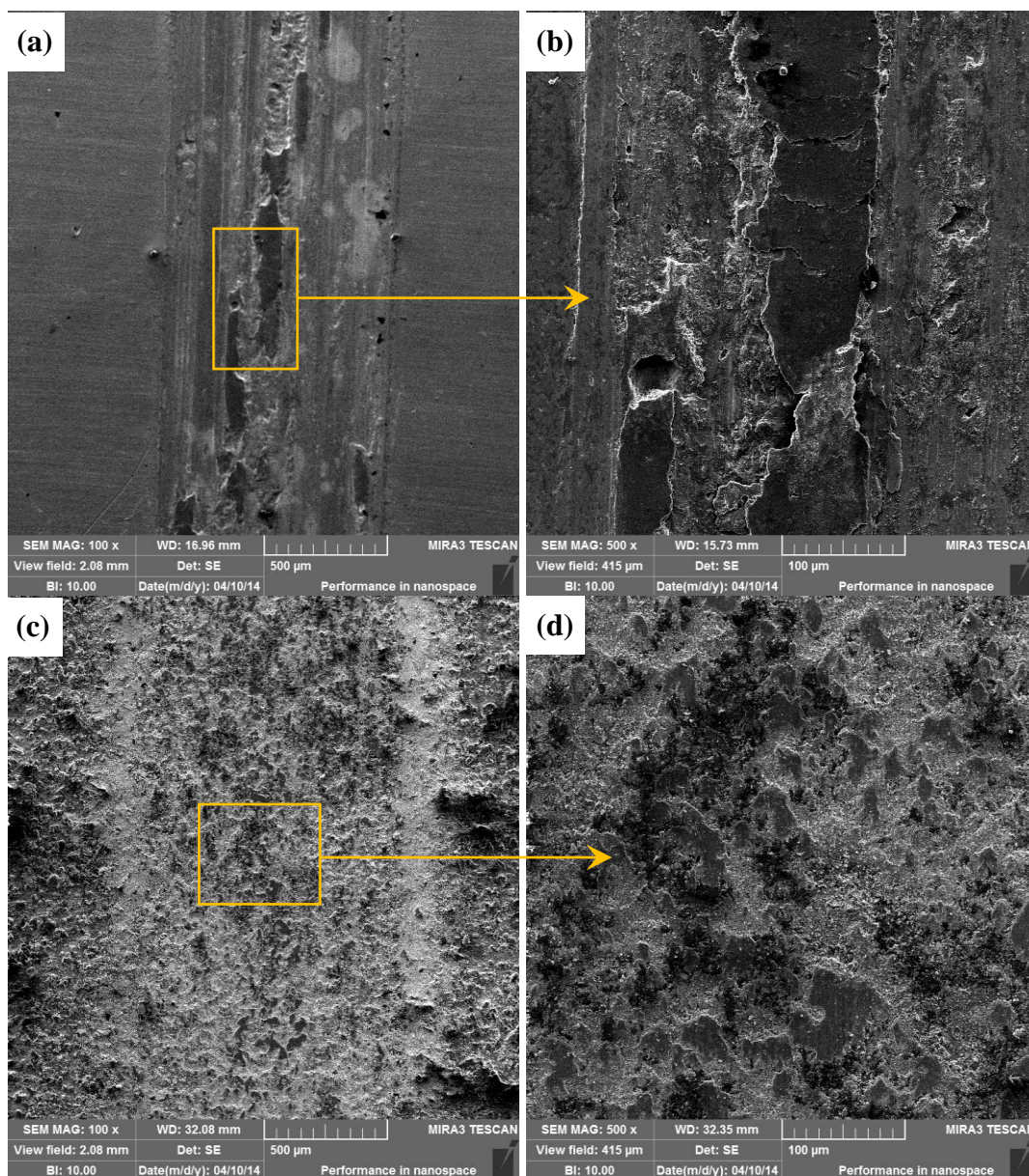


Figure 4. Wear scars of boronizing coating and P110 substrate-against GCr15: (a) P110 substrate in lower magnification; (b) P110 substrate in higher magnification; (c) boronizing coating in lower magnification; (d) boronizing coating in higher magnification

Figure 5a suggests the wear scar of P110 steel against Si_3N_4 , the wear scar is continuous. Figure 5b shows the high magnified image of Figure 5a, it is evident that many grooves are parallel to the sliding direction. Hence the main wear manner of P110 steel under this condition can be judged as severe abrasive wear. Figure 5c displays the whole feature of the wear scar of boronizing coating; it is

notable that the dark area is narrower than that of P110 steel. Nevertheless, wear debris can be observed under the higher magnification worn surface in Figure 5d. The predominant wear manner of boronizing coating can be deduced as slight abrasive wear.

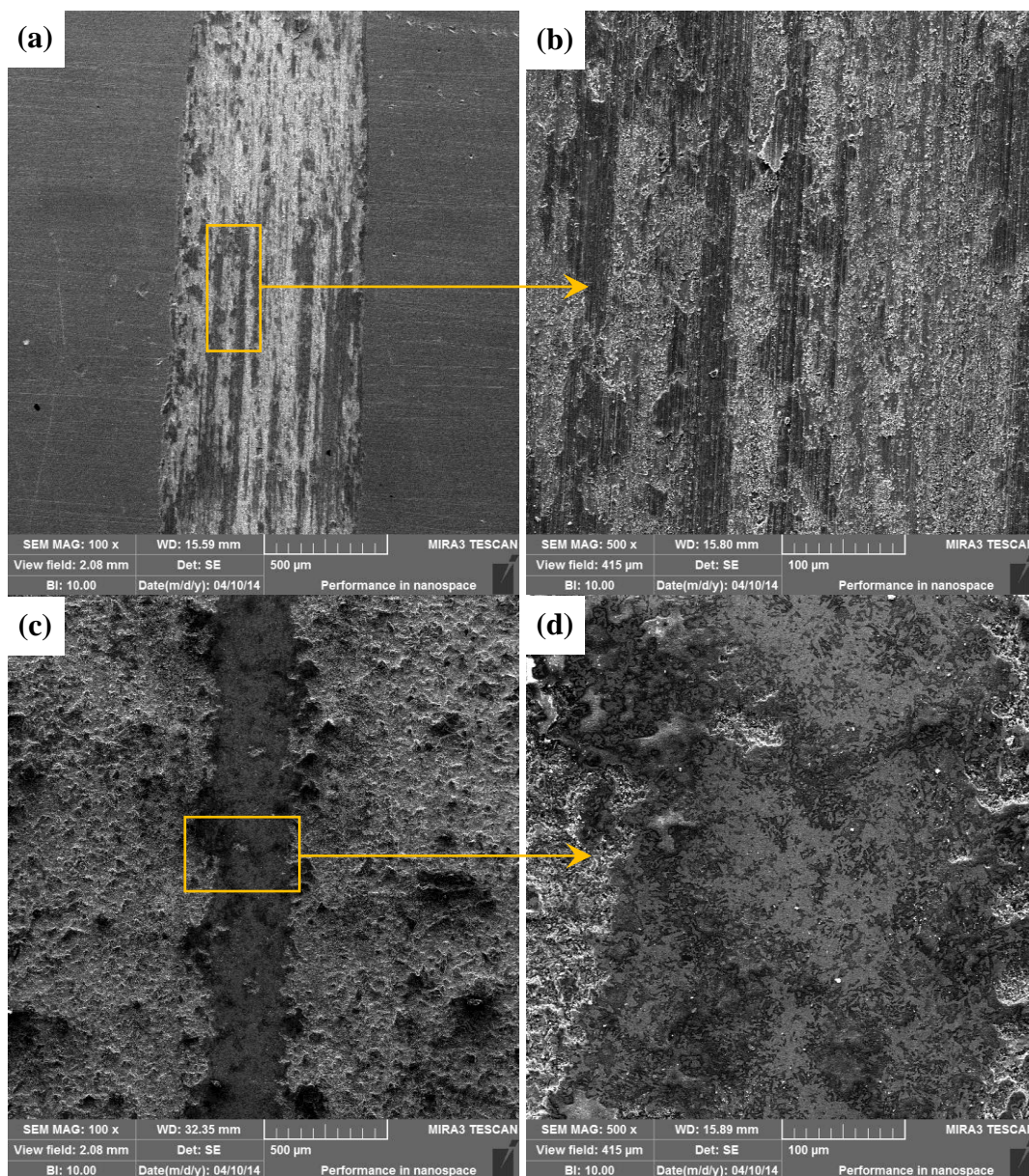


Figure 5. Wear scars of boronizing coating and P110 substrate-against Si_3N_4 : (a) P110 substrate in lower magnification; (b) P110 substrate in higher magnification; (c) boronizing coating in lower magnification; (d) boronizing coating in higher magnification

Seen from the mass loss figure of P110 steel and boronizing treated coating after sliding against GCr15 (Figure 6a), the mass of P110 steel decreases 0.750 mg while the composite coating mass increases 0.100 mg, which confirmed the adhesive transfer of counterpart material. This phenomenon represents better wear resistance performance of the boronizing coating. Figure 6b compares the mass variation of the P110 steel and boronizing coating after dry sliding against Si_3N_4 . It is notable that the

mass loss of the boronizing coating (0.120 mg) is lower than P110 steel (0.700 mg). The smaller reduction amount derives from the enhancement in surface hardness of the coating.

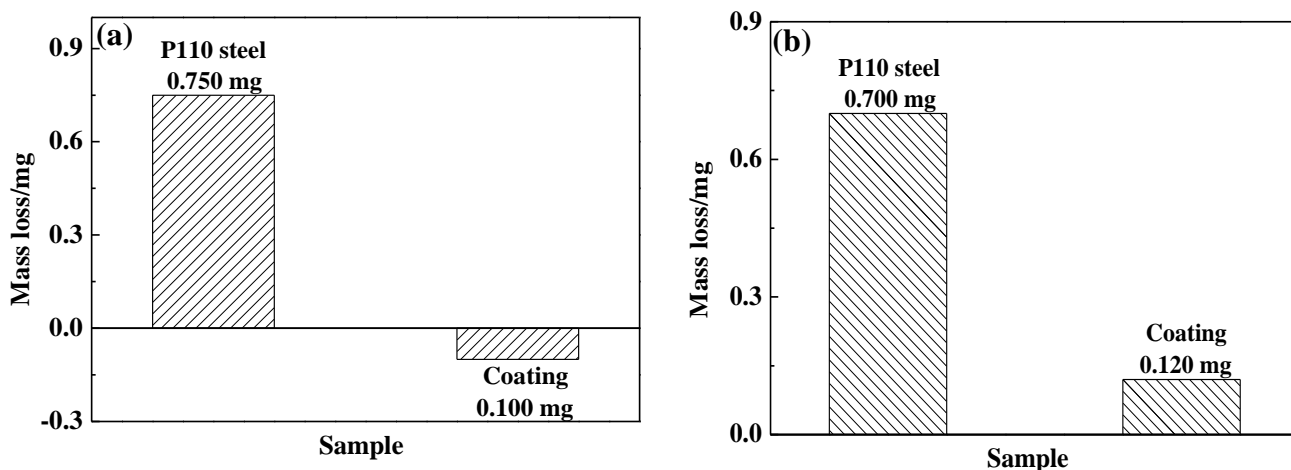


Figure 6. Column charts of mass losses to tested samples after sliding against (a) GCr15 and (b) Si₃N₄

3.4. Corrosion resistance of boronizing coating

The measurement of the OCP was chosen to evaluate the chemical stability and corrosion process of the experimental samples [15, 16]. The change of OCP is also assumed to be related to the growth and stability of the corrosion scale on the testing material surface [15]. The OCP scans of the tested samples as a function of elapsed time were recorded after each testing sample was put into the in electrolytic cells, and the testing time was 3600 s.

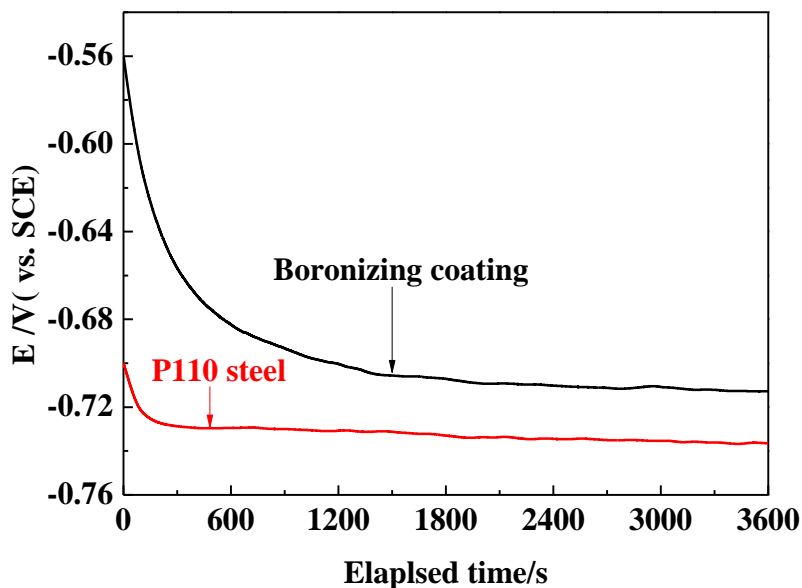


Figure 7. E_{ocp} vs. time curves of the boronizing coating and P110 steel in oilfield brine

Figure 7 illustrates the comparative studies on OCPs of the boronizing coating and P110 steel. It is obvious that the OCP value of boronizing coating (-0.71 V) is higher than P110 steel (-0.73 V) as expected. This confirms that the boronizing coating improves the chemical stability against corrosion of P110 steel in simulated oilfield stratum water.

In order to compare the corrosion resistance of P110 steel substrate and treated boronizing coating, potentiodynamic polarization measurements were conducted in the same solutions.

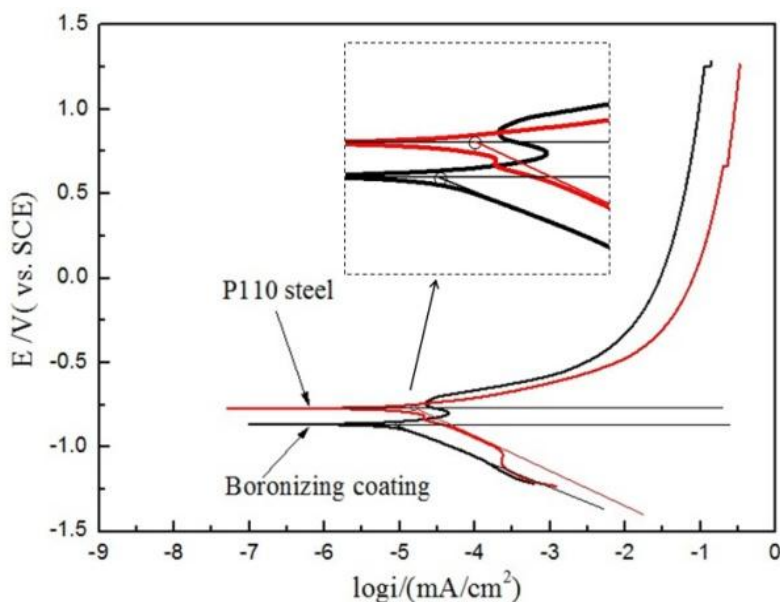


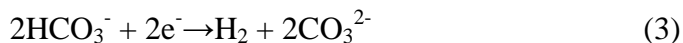
Figure 8. Polarization curves of the boronizing coating and the P110 steel

The anodic and cathodic plots of the specimens were studied after OCP measurements at a scan rate of 1 mV s^{-1} , and the voltage scanning range was $-0.5 \sim 2.0 \text{ V}$ versus OCP. Representative polarization curves of the treated coating and P110 steel are shown in Figure 8. The corrosion potential (E_{corr}) is the voltage difference between the tested sample immersed in a given medium and an appropriate SCE. The more negative E_{corr} is, the more the corrosion tendency is [17, 18]. Compared to P110 steel, the boronizing coating has presented more negative corrosion potential, but has indicated lower corrosion current density. The corrosion current density is responsible for the corrosion rate, higher current density signals higher corrosion rate during polarization measurement. The corrosion current density in Table 3 of each sample was calculated by Tafel extrapolation method from the polarization curves. It can be found that the P110 steel has a corrosion current density (i_{corr}) of $1.56675\text{E-}05 \text{ A/cm}^2$, which is higher than the boronizing coating of $8.74984\text{E-}06 \text{ A/cm}^2$ in simulated stratum water. The corrosion current density is commonly cited as an important criterion to evaluate the kinetics of corrosion process. The corrosion rate is normally proportional to the corrosion current density. The lower corrosion current density of boronizing coating confirms the improvement in corrosion resistance for P110 steel.

It is acknowledged that when the CO_2 dissolved into water and formed the carbonic acid, the reaction is shown in Equation (1):



The carbonic acid is even more corrosive to steel than a completely dissociated acid at the same pH value, which can be reflected by the following cathodic reactions, as given in Equations 2-4 [19]:



The anodic reactions are suggested in Equations 5-8:



As shown in Figure 8, P110 steel suggests no obvious passivation. The boronizing coating has revealed a narrow passive region around 0 V (SCE). By increasing the potential from the corrosion potential within the passive region, the current density decreases slightly due to the protective barrier effect. The boronizing coating can protect the P110 steel from corrosion attack.

The EIS measurements were recorded after immersion in the test solution for 3600 s. Figure 9 shows the detailed Nyquist plots of the P110 steel and boronized coating. Each impedance spectra consist of a capacitive loop, which is related to the charge transfer of the corrosion process occurred on the surface of the tested sample. The diameters of the arcs in the Nyquist plots could basically illustrate the corrosion resistance of test samples. It is clear that the semicircle diameter of the treated boronizing coating in the Nyquist plot is far bigger than that of the substrate, which indicates that the coating can greatly improve the surface corrosion resistance of the substrate P110 steel.

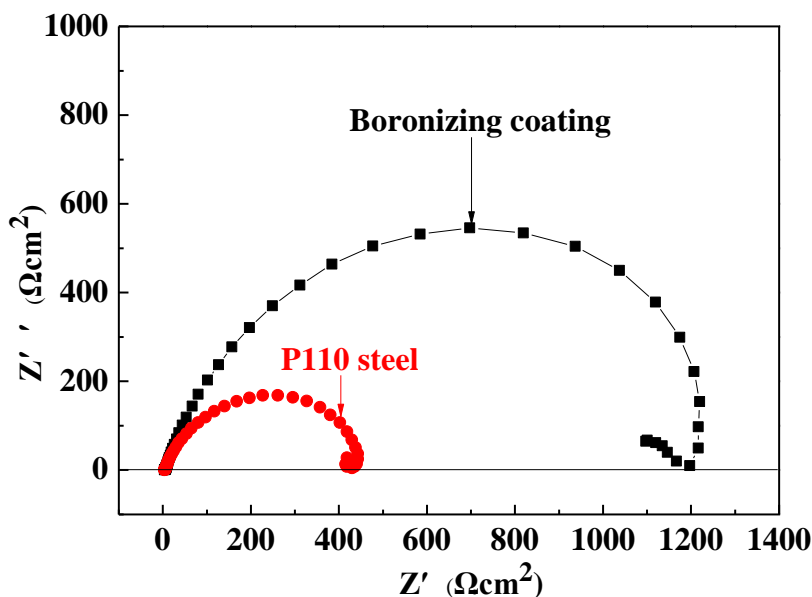


Figure 9. Nyquist plots of the ESD coating and P110 steel

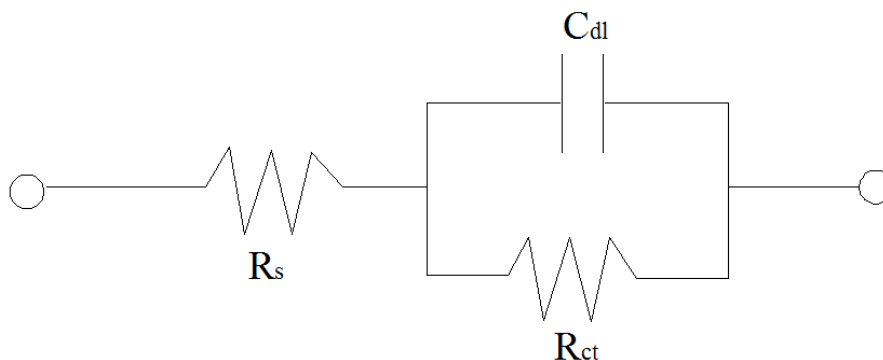


Figure 10. Equivalent electrical circuit model

Impedance data were analyzed using Zplot and ZView software and values of charge transfer resistance R_{ct} , solution resistance R_s and double-layer capacitance C_{dl} were determined using an electrical equivalent circuit. An equivalent electrical circuit model given in Figure 10 has been used to simulate the metal/solution interface and to analyze the Nyquist plots. The charge transfer resistance R_{ct} and double layer capacitance C_{dl} obtained for the substrate and boronizing coating are compiled in Table 3. The value of R_{ct} is a measure of the electron transfer across the surface and is inversely proportional to corrosion rate. The higher R_{ct} value of boronizing coating implies a good corrosion protective ability for the bare sample. The C_{dl} value may be related to the porosity of the coating. The low C_{dl} value confirms that the boronizing coating is relatively less porous in nature [16, 20]. The protective effect of the boronizing coating on P110 steel calculated from EIS is in good agreement with that obtained from potentiodynamic polarization.

Table 3. Electrochemical test results of the tested samples in the corrosion media

Sample	Potentiodynamic polarization				EIS	
	E_{OCP}/V	$\beta_c(mv/dec)$	$\beta_a(mv/dec)$	$i_{corr}/A \cdot cm^{-2}$	$C_{dl}/\mu F \cdot cm^2$	$R_{ct}/\Omega \cdot cm^2$
P110 steel	-0.71	189	108	1.56675E-05	1333.27	471.9
Boronizing coating	-0.73	182	176	8.74984E-06	113.36	4058.6

4. LIMITATIONA AND FUTURE WORK

Material engineers are constantly confronted with the challenge to design and produce new materials that can both resistant wear and corrosion over wide range of modern industrial environments. The oil casing tube which is an important structural unit of the oil/gas well, usully simultaneously suffers wear and corrosion practical applications. By this reason, the adopted surface protection technology is expected to endow the material with improved wear and corrosion resistance. Fortunately the boronizing can meet the demand with low cost. Boronizing is versatile owing to its unique properties such as uniformity on complex geometrical components, resistance to wear and corrosion. It is well known that an oil well is usually thousands miles in depth, the casing tubes are connected by collars in the oil well (see Figure 1 and Figure 11) [4, 21, 22]. Of course the tubing collars play an important role in ensuring the service safety of casing tubes. Due to the adverse factors,

such as the length of a casing tube and the capacity of the vacuum chamber, it is difficult to achieve the boronizing treatment of whole casing tubes. However, it is realistic to batch boronizing of tubing collars and realize surface strengthening. The present preliminary results seem promising and it is also needed to carry out further experiments and investigations to obtain an optimal processing parameter for practical application.

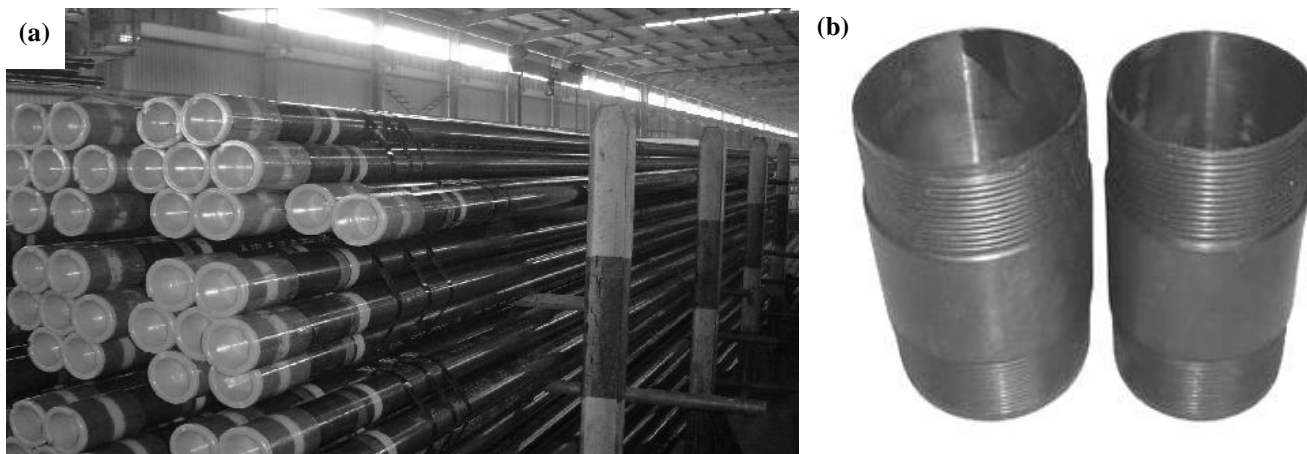


Figure 11. Pictures of oil casing tube (a) and tubing collar (b).

5. CONCLUSION

Continuous boronizing coating was synthesized on P110 steel by pack cementation. The obtained coating mainly consisted of Fe_2B and reached a thickness of $20\ \mu\text{m}$. In dry sliding against GCr15, the wear mechanism of P110 steel was abrasive wear combined with adhesive wear; the wear mode of boronizing coating was mainly the adhesive transfer of GCr15 ball. In dry sliding against Si_3N_4 , the main wear manner of P110 steel was abrasive wear; the predominant wear manner of boronizing coating was deduced as slight wear and abrasive wear. The boronizing coating showed higher corrosion resistance than that of P110 steel in simulated oilfield stratum water indicated by its electrochemical measurements results.

ACKNOWLEDGEMENTS

This work was supported by the National Natural Science Foundation of China (51208333), the China Postdoctoral Science Foundation (No.2012M520604), the Natural Science Foundation for Young Scientists of Shanxi Province (No.2013021013-2, No. 2014011036-1), the Youth Foundation of Taiyuan University of Technology (No.2012L050, No.2013T011) and the Qualified Personnel Foundation of Taiyuan University of Technology (QPFT) (No.tyut-rc201157a).

References

1. M. Finšgar, *Corros. Sci.* 86 (2014) 17.
2. H.L. Li, Y.P. Zhang, L.H. Han, *Steel Pipe* 36 (2007) 1.
3. H.L. Li, Y.P. Zhang, L.H. Han, *Steel Pipe* 37 (2008) 1.

4. N.M. Lin, M.L. Li, J.J. Zou, X.G. Wang, B Tang, *J. Mater. Eng. Perform.* 22 (2013) 1365.
5. X.F. Wu, Y.H. Lin, C.W. Wu, T.H. Shi, R.F. Li, T.J. Lin, *J. Southwest Petrol. Inst.* 26 (2004) 65.
6. N.M. Lin, F.Q. Xie, H.J. Yang, W. Tian, H.F. Wang, B Tang, *Appl. Surf. Sci.* 258 (2012) 4960.
7. J.J.Zou, N.M. Lin, L. Qin, B. Tang, F.Q. Xie, *Surf. Rev. Lett.* 20 (2013) 1330002–1.
8. Z.G. Su, X. Tian, J. An, Y. Lu, Y.L. Yang, S.J. Sun, *ISIJ Inter.* 49 (2009) 1776.
9. A. Çalik, *ISIJ Inter.* 53 (2013) 160.
10. P. Juijerm, *Kovové Mater.* 52 (2014) 231.
11. N.M. Lin, F.Q. Xie, J. Zhou, T. Zhong, X.Q. Wu, W. Tian, *J. Cent. South Univer.* 17 (2010) 1151.
12. N.M. Lin, F.Q. Xie, J. Zhou, X.Q. Wu, W. Tian, *J. Wuhan Univer. Technol. Mater. Sci. Ed.* 26 (2011) 191.
13. S.M. Sherif E., A.A. Almajid, *Int. J. Electrochem. Sci.* 10 (2015) 34.
14. V.V. Medeliene, A. Stankevič, A. Grigucevičiene, A. Selskiene, G. Bikulčius, *Mater. Sci.* 17 (2011) 132.
15. H. Mindivan, *Kovové Mater.* 48 (2010) 203.
16. N.M. Lin, H.Y. Zhang, J.J. Zou, P.J. Han, Y. Ma, B. Tang, *Int. J. Electrochem. Sci.* 10 (2015) 356.
17. Z.J. Liu, X.H. Liu, U. Donatus, G.E. Thompson, P. Skeldon, *Int. J. Electrochem. Sci.* 9 (2015) 3558.
18. Z.M. Gao, S. Zhao, Y. Wang, X. Wang, L.J. Wen, *Int. J. Electrochem. Sci.* 10 (2015) 637.
19. J. K. Heuer, J. F. Stubbins, *Corros. Sci.* 41 (1999) 1231.
20. A.M. Atta, G. A. El-Mahdy, H. A. Allohedan, S.M. El-Saeed, *Int. J. Electrochem. Sci.* 10 (2015) 8.
21. <http://www.wsphl.com/tg.asp>.
22. <http://free.99114.com/SupplyDetail/297032/986824.shtml>.

© 2015 The Authors. Published by ESG (www.electrochemsci.org). This article is an open access article distributed under the terms and conditions of the Creative Commons Attribution license (<http://creativecommons.org/licenses/by/4.0/>).